

Electronic supplementary information

Tailoring Molecular Geometry of Polyfluoride Perylene Diimide Acceptor towards Efficient Organic Solar Cells

Yan Wang,^a Hongbin Zhong,^{*b} Yuwen Hong,^a Tong Shan,^a Kui Ding,^a Lei Zhu,^a Feng Liu,^a Hao Wei,^{*a} Chunyang Yu^{*a} and Hongliang Zhong^{*a}

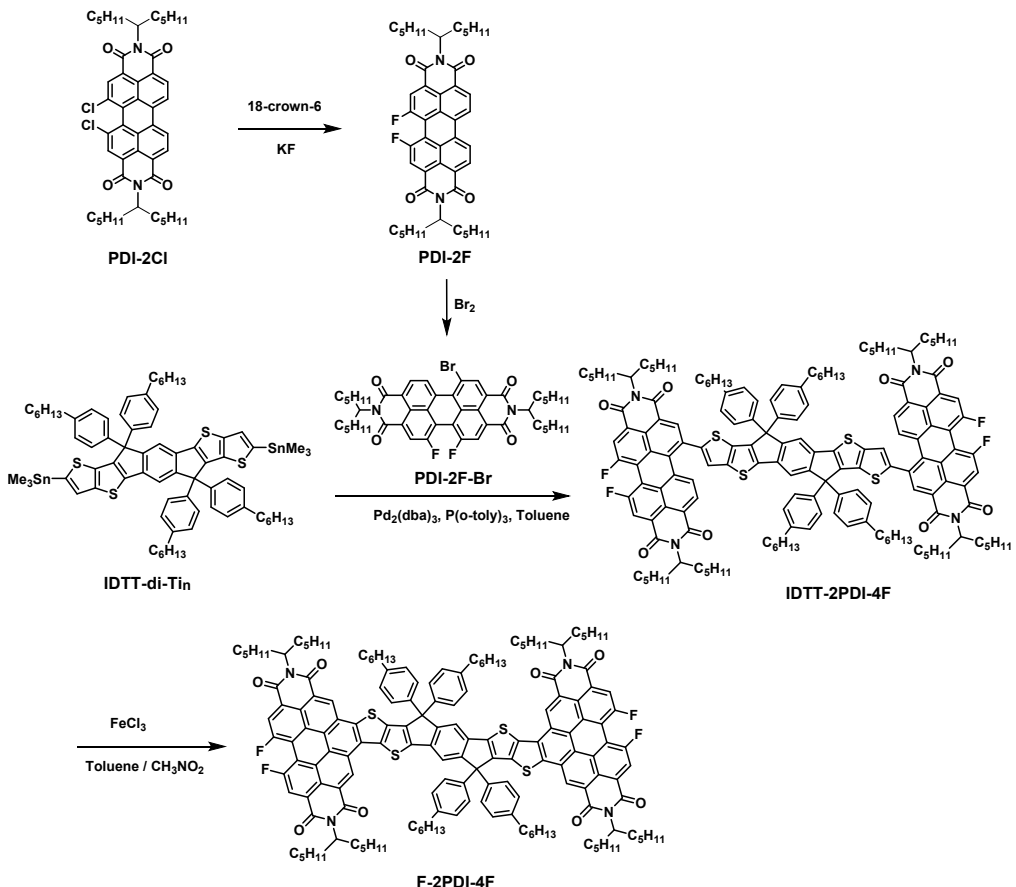
^aSchool of Chemistry and Chemical Engineering, Key Laboratory for Thin Film and Micro-fabrication Technology of Ministry of Education, Shanghai Jiao Tong University, Shanghai 200240, China. E-mail: haowei@sjtu.edu.cn; chunyangyu@sjtu.edu.cn; hlzhong@sjtu.edu.cn.

^bHunan Provincial Key Laboratory of Fine Ceramics and Powder Materials, School of Materials and Environmental Engineering, Hunan University of Humanities, Science and Technology, Loudi, 417000, China. E-mail: hbzhong@huhst.edu.cn.

1. Instruments and measurements

¹H and ¹³C NMR spectra were measured by Bruker Avance-III HD 400 and Avance-III HD 500 spectrometer using *d*-chloroform (CDCl₃) as the solvent and tetramethylsilane (TMS) as internal standard at room temperature, respectively. Matrix-assisted laser desorption/ionization time of flight mass spectrometry (Maldi-Tof-MS) was measured by Bruker autoflex speed TOF/TOF with dichloromethane (CH₂Cl₂) at reflection mode utilizing DCTB (trans-2-[3(4-tert-butylphenyl)-2-methyl-2-propenyl]malononitrile) as matrix. UV-Vis absorption spectroscopy (UV-Vis) were recorded on a Lambda 750S UV-Vis spectrophotometer with dilute solution in chloroform or film. Electrochemical cyclic voltammetry (CV) was tested by a CHI660D electrochemical workstation at room temperature. The geometry of F-2PDI and F-2PDI-4F was optimized via Gaussian 09 software using density functional theory (DFT) at ω B97X-D/6-31G(d,p) level to provide rational and convincing theoretical results. The hexyl side chains of F-2PDI and F-2PDI-4F were replaced by methyl groups to simplify the calculation. Atomic force microscopy (AFM) measurement was conducted on a Bruker Multimode 8 in tapping mode. Transmission electron microscopy (TEM) measurement was conducted on a Talos L120C G2 from Thermo Fisher Scientific. The characterization of GIWAXS for the blend films was obtained from the Advanced Light Source (Lawrence Berkeley National Laboratory) on beamline 7.3.3. The incident angle and the beam energy were 0.16° and 10 keV, respectively. The samples were spin-coated on the Si/PEDOT:PSS substrates in optimized conditions.

2. Synthesis



Scheme S1. Synthetic route of F-2PDI-4F.

The F-2PDI was synthesized according to the reference.^{1, 2}

Synthesis of PDI-2F. The mixture solution of **PDI-2Cl** (1.00 g, 1.30 mmol) and **KF** (8.74 mmol) in 80 mL dry DMF was heated to 160 °C and kept stirring for 0.5 h, followed by the addition of 18-crown-6 (0.17 g, 0.65 mmol). The solution was kept vigorous stirring at 160 °C for 8 h. The reaction solution was cooled to room temperature and then poured into 1 L H₂O. After filtration, the precipitate was washed by water. The crude product was purified by silica gel column chromatography column chromatography on silica gel (petroleum ether:CH₂Cl₂, 1:1 to 1:2 v/v) to afford **PDI-2F** (267mg, yield: 28%). as a red solid. ¹H NMR (400 MHz, CDCl₃) δ: 8.65 (m, 4H), 8.48 (m, 2H), 5.24- 5.12 (m, 2H), 2.31-2.17 (m, 4H), 1.85 (m, 4H), 1.35-1.19 (m, 24H), 0.83 (m, 12H). ¹³C NMR (100 MHz, CDCl₃) δ: 164.59, 163.76, 162.73, 133.89, 130.84, 130.14, 128.56, 126.03, 123.77, 123.04, 122.73, 117.13, 55.16, 32.39, 31.85, 29.85, 26.72, 22.69, 14.17. ¹⁹F NMR (376 MHz, CDCl₃) δ: -92.31 (s). MS (MALDI-TOF) m/z: Calculated for C₄₆H₅₂F₂N₂O₄, 735.39; Found, 735.27.

Synthesis of PDI-2F-Br. Bromine (10.66 g, 13.60 mmol) was added slowly **PDI-2F** (1.00 g, 0.14 mmol) in 60 mL dichloromethane. The mixture solution was stirred in

dark at room temperature for 5 h. The excess of bromine was quenched by aqueous Na₂SO₃ solution, followed by the extraction of dichloromethane. The organic phase was dried by anhydrous Na₂SO₄ and the solvent was removed under vacuum. The crude product was purified by column chromatography on silica gel (petroleum ether:CH₂Cl₂, 1:1 v/v) to give **PDI-2F-Br** (0.95 g, yield: 86%) as a red solid. ¹H NMR (400 MHz, CDCl₃) δ: 9.55 (d, *J* = 8.2 Hz, 1H), 8.91 (s, 1H), 8.68 (s, 1H), 8.48 (s, 2H), 5.23-5.09 (m, 2H), 2.30-2.17 (m, 4H), 1.91-1.79 (m, 4H), 1.39-1.19 (m, 24H), 0.84 (m, 12H). ¹³C NMR (100 MHz, CDCl₃) δ: 164.30, 163.51, 162.64, 160.60, 158.09, 137.95, 137.33, 134.53, 134.02, 133.56, 132.73, 132.56, 130.70, 129.56, 129.00, 128.71, 127.80, 126.10, 125.09, 124.22, 123.09, 121.86, 121.32, 116.83, 115.94, 55.37, 55.17, 32.40, 32.33, 31.85, 31.82, 26.71, 26.88, 22.69, 14.17. ¹⁹F NMR (376 MHz, CDCl₃) δ: -94.57 (s), -94.76 (s). MS (MALDI-TOF) m/z: Calculated for C₄₆H₅₁F₂N₂O₄Br, 813.30; Found, 813.26.

Synthesis of IDTT-2PDI-4F: IDTT-di-Tin (0.22g, 0.16 mmol), PDI-2F-Br (0.30g, 0.37 mmol), Pd₂(dba)₃ (6.6mg, 0.006 mmol) and P(*o*-Tol)₃ (7.8 mg, 0.026 mmol) were dissolved in 15 mL toluene under argon. Then, the mixture was kept reflux overnight. After cooling to room temperature, the crude product was extracted with dichloromethane and washed with water. The organic phase was dried by anhydrous Na₂SO₄ and the solvent was removed under vacuum. The crude product was purified by silica gel column chromatography (petroleum ether:CH₂Cl₂, 2:1 v/v), affording a black solid (0.32g, yield: 81%). ¹H NMR (400 MHz, CDCl₃) δ: 8.70 (m, 2H), 8.46 (m, 4H), 8.32 (m, 2H), 8.22 (m, 2H), 7.58 (s, 2H), 7.52 (s, 2H), 7.16 (d, *J* = 8.3 Hz, 8H), 7.10 (d, *J* = 8.3 Hz, 8H), 5.15 (m, 4H), 2.58 (m, 8H), 2.25 (m, 8H), 1.93-1.79 (m, 8H), 1.61 (m, 8H), 1.35-1.21 (m, 72H), 0.87-0.82 (m, 36H). ¹³C NMR (100 MHz, CDCl₃) δ: 163.97, 163.04, 160.37, 153.83, 146.84, 145.02, 144.20, 143.94, 142.39, 142.33, 139.92, 136.26, 135.55, 134.59, 130.43, 130.01, 128.76, 128.06, 125.47, 124.94, 121.76, 121.19, 117.56, 63.12, 55.09, 35.72, 32.38, 31.88, 31.84, 31.52, 29.38, 26.68, 22.76, 22.71, 14.24, 14.22, 14.18. ¹⁹F NMR (376 MHz, CDCl₃) δ -94.38, -94.75, -95.04, -95.45. MS (MALDI-TOF) m/z: Calculated for C₁₆₀H₁₇₄F₄N₄O₈S₄, 2484.22; Found, 2484.65.

Synthesis of F-2PDI-4F: IDTT-2PDI-4F (0.23g, 0.09 mmol) was dissolved in 60 mL dry toluene, followed by the addition of a solution of FeCl₃ (0.22g, 0.139 mmol) in 0.2 mL CH₃NO₂. The mixture is heated to 45 °C and kept stirring for 30 min. After cooling to room temperature, the product was poured into methanol. The crude product was filtrated and washed with methanol. The crude product was purified by silica gel column chromatography (petroleum ether:CH₂Cl₂, 2:1 v/v), yielding a deep green solid (0.16g, 70%). ¹H NMR (400 MHz, CDCl₃) δ: 9.97 (br, 2H), 9.58 (br, 2H), 8.80 (br, 4H), 7.91 (s, 2H), 7.42 (d, 8H), 7.28 (d, 8H), 5.34 (m, 4H), 2.71-2.58 (m, 8H), 2.37 (m, 8H), 1.96 (m, 8H), 1.68 (m, 8H), 1.44-1.25 (m, 72H), 0.86 (m, 36H). ¹³C NMR (125 MHz, CDCl₃) δ 164.97, 164.20, 163.11, 154.71, 147.72, 147.29, 142.61, 142.64, 142.24, 149.75, 136.99, 136.57, 135.26, 131.33, 129.15, 128.19, 127.11, 124.50, 123.53, 122.90, 122.01, 118.15, 117.12, 68.13, 63.79, 55.48, 35.83, 32.57, 31.93, 31.88, 31.43, 29.31, 26.91, 26.83, 25.79, 2275, 22.74, 22.73, 14.22. ¹⁹F NMR (376 MHz, CDCl₃) δ -90.83. MS (MALDI-TOF) m/z: Calculated for C₁₆₀H₁₇₀F₄N₄O₈S₄, 2480.18; Found, 2480.07.

Table S1. The screening D/A ratio and additives of PTB7-Th:F-2PDI based devices.

PTB7-Th:F-2PDI	V_{oc} (V) ^a	J_{sc} (mA cm ⁻²) ^a	FF (%) ^a	PCE (%) ^a
D:A = 1:0.8	1.00±0.01	10.20±0.03	49.0±0.4	4.96±0.08 (5.03)
D:A = 1:1.0	1.00±0.01	10.50±0.02	52.0±0.1	5.46±0.02 (5.48)
D:A = 1:1.2	1.00±0.01	11.67±0.02	51.0±0.3	5.95±0.03 (5.98)
D:A = 1:1.5	1.00±0.01	11.00±0.05	50.8±0.4	5.59±0.03 (5.62)
As-cast	1.00±0.01	11.67±0.02	51.0±0.3	5.95±0.03 (5.98)
+1.0 vt% CN	1.01±0.01	12.91±0.02	51.7±0.6	6.74±0.07 (6.80)
+2.0 vt% CN	1.02±0.01	13.22±0.13	53.9±0.9	7.27±0.14 (7.44)
+3.0 vt% CN	1.02±0.01	13.14±0.12	51.2±0.9	6.86±0.12 (6.95)
+1.0 vt% DIO	1.00±0.01	11.96±0.02	51.0±0.3	6.10±0.03 (6.13)

^aThe average values and standard deviations in parentheses are statistical data from ten independent cells. CN represents 1-chloronaphthalene and DIO represents 1,8-diiodooctane.

Table S2. The screening D/A ratio and additives of PTB7-Th:F-2PDI-4F based devices.

PTB7-Th:F-2PDI-4F	V_{oc} (V) ^a	J_{sc} (mA cm ⁻²) ^a	FF (%) ^a	PCE (%) ^a
D:A = 1:1.0	0.94±0.01	9.76±0.04	45.0±0.2	4.13±0.02 (4.15)
D:A = 1:1.5	0.94±0.01	10.92±0.12	44.1±0.1	4.53±0.08 (4.60)
D:A = 1:2.0	0.93±0.02	9.55±0.08	43.9±0.5	3.90±0.10 (3.96)
As-cast	0.94±0.01	10.92±0.12	44.1±0.1	4.53±0.08 (4.60)
+2.0 vt% CN	0.95±0.01	11.90±0.18	46.0±0.4	5.20±0.04 (5.27)

^aThe average values and standard deviations in parentheses are statistical data from ten independent cells.

Table S3. The screening D/A ratio and additives of PBDB-T:F-2PDI based devices.

PBDB-T:F-2PDI	V_{oc} (V) ^a	J_{sc} (mA cm ⁻²) ^a	FF (%) ^a	PCE (%) ^a
D:A = 1:0.8	1.03±0.01	11.22±0.04	58.2±0.2	6.73±0.02 (6.75)
D:A = 1:1.0	1.02±0.01	11.48±0.02	56.3±0.1	6.29±0.03 (6.33)
As-cast	1.03±0.01	11.22±0.04	58.2±0.2	6.73±0.02 (6.75)
+0.5 vt% DIO	1.03±0.01	11.23±0.04	60.4±0.5	6.99±0.06 (7.07)
+1.0 vt% DIO	1.03±0.01	10.95±0.06	60.2±0.4	6.79±0.05 (6.85)

^aThe average values and standard deviations in parentheses are statistical data from ten independent cells.

Table S4. The screening D/A ratio, additives and TA of PBDB-T:F-2PDI-4F based devices.

PBDB-T:F-2PDI-4F	V_{oc} (V) ^a	J_{sc} (mA cm ⁻²) ^a	FF (%) ^a	PCE (%) ^a
D:A = 1:0.6	1.00±0.01	12.99±0.03	65.2±0.4	8.47±0.06 (8.52)
D:A = 1:0.8	1.00±0.01	13.28±0.03	64.7±0.1	8.59±0.04 (8.61)
D:A = 1:1.0	1.00±0.01	12.75±0.03	63.5±0.6	8.09±0.04 (8.11)
D:A = 1:1.2	1.00±0.01	12.91±0.02	62.0±0.1	8.01±0.02 (8.03)
As-cast	1.00±0.01	13.28±0.03	64.7±0.1	8.59±0.04 (8.61)
+0.5 vt% CN	1.00±0.01	11.50±0.02	63.9±0.6	7.06±0.07 (7.11)
+1.0 vt% CN	1.01±0.01	9.71±0.18	50.9±0.6	4.99±0.04 (5.03)
+0.5 vt% DIO	1.00±0.01	13.42±0.07	66.1±0.8	8.96±0.10 (9.05)
+1.0 vt% DIO	1.00±0.01	13.51±0.09	64.5±0.7	8.72±0.09 (8.79)
w/o TA	1.00±0.01	13.38±0.06	66.6±0.6	8.92±0.05 (9.03)
90°C TA	1.00±0.01	13.54±0.05	65.7±0.7	8.90±0.09 (8.98)

^aThe average values and standard deviations in parentheses are statistical data from ten independent cells. TA represents thermal annealing for 10 min.

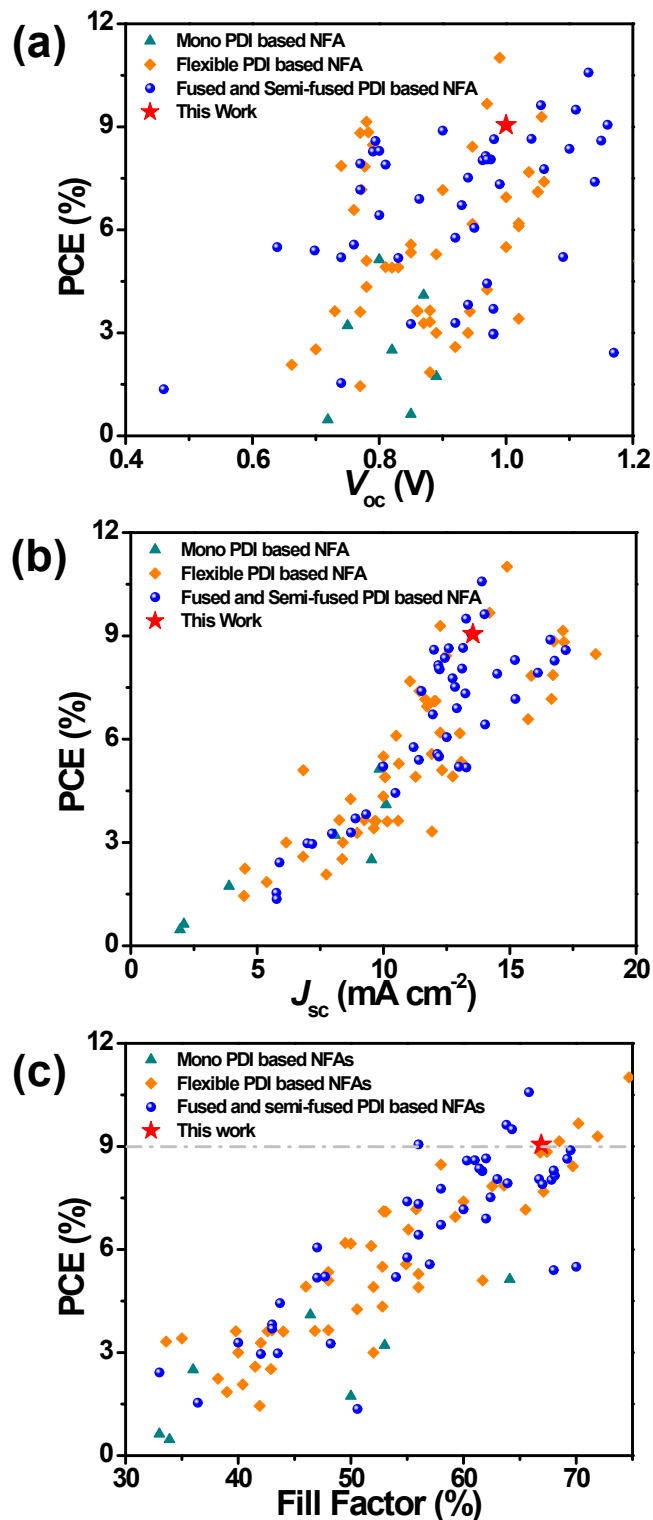


Fig. S1. Plots of (a) V_{oc} , (b) J_{sc} and (c) FF versus PCEs of the reported efficient OSCs with PDI-based NFAs¹⁻⁵⁴.

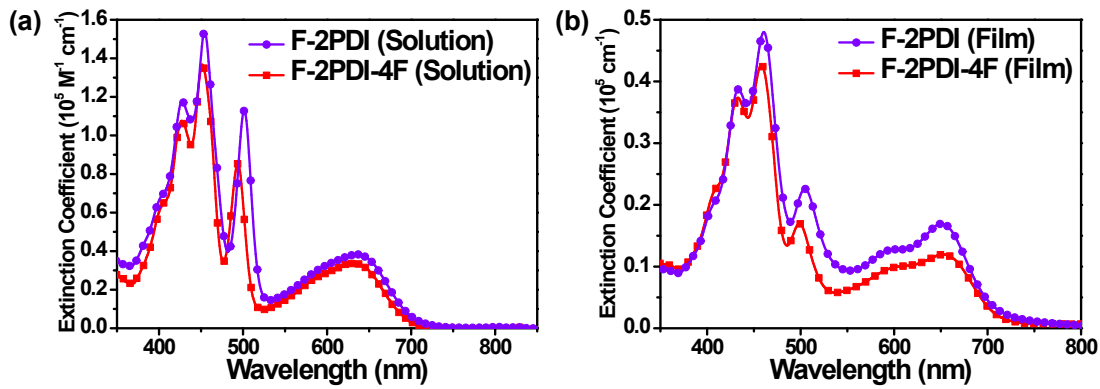


Fig. S2. UV-vis absorption spectra of F-2PDI and F-2PDI-4F (a) in chloroform solution and (b) in film.

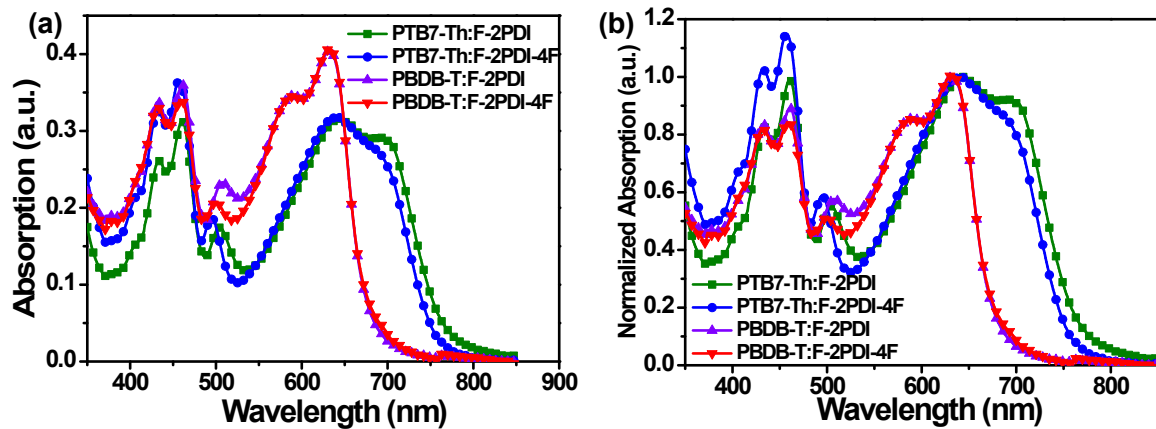


Fig. S3. (a) Absorption spectra and (b) normalized absorption spectra of varied active layers.

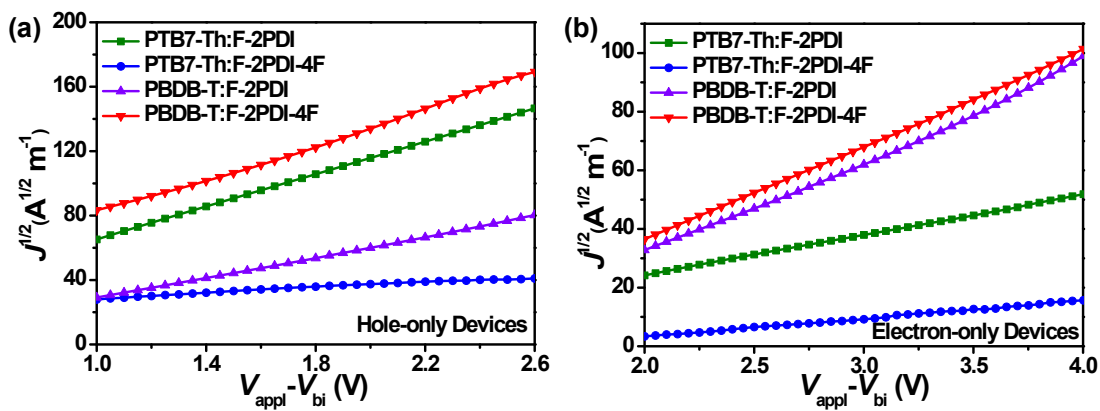


Fig. S4. Plots of $J^{1/2}$ as a function of $V_{\text{appl}} - V_{\text{bi}}$ for the (a) hole-only devices and (b) electron-only devices based on varied active layers.

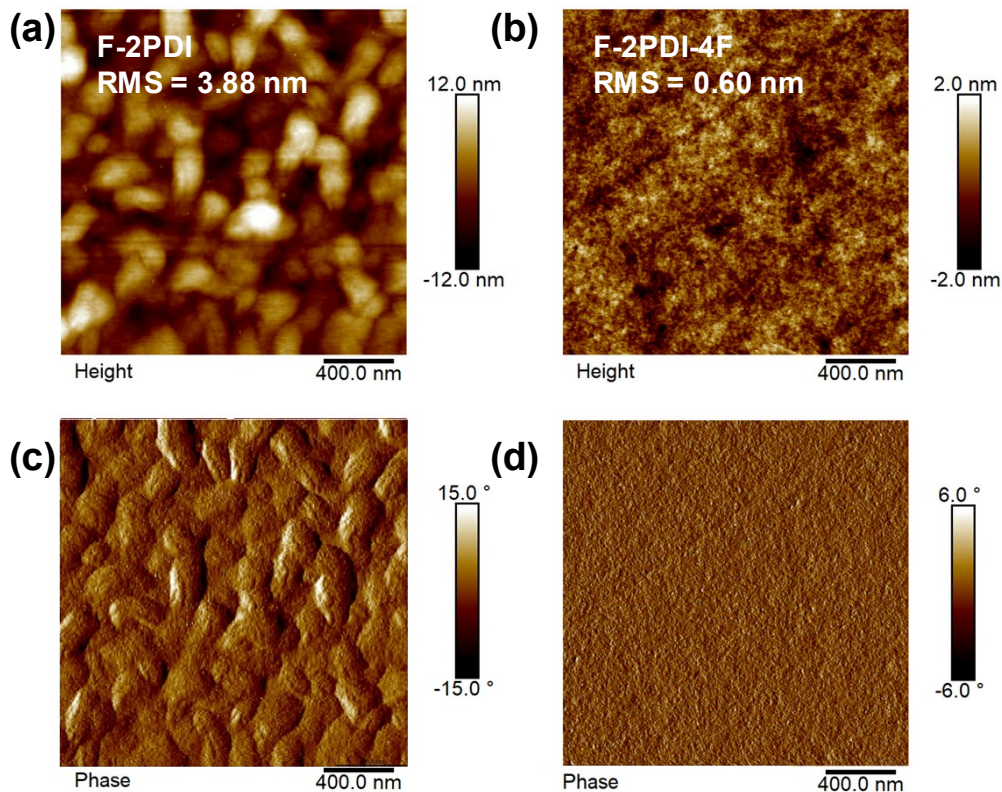


Fig. S5. Tapping-mode AFM height and phase images ($2 \times 2 \mu\text{m}$) of neat films based on F-2PDI (a, c), F-2PDI-4F (b, d).

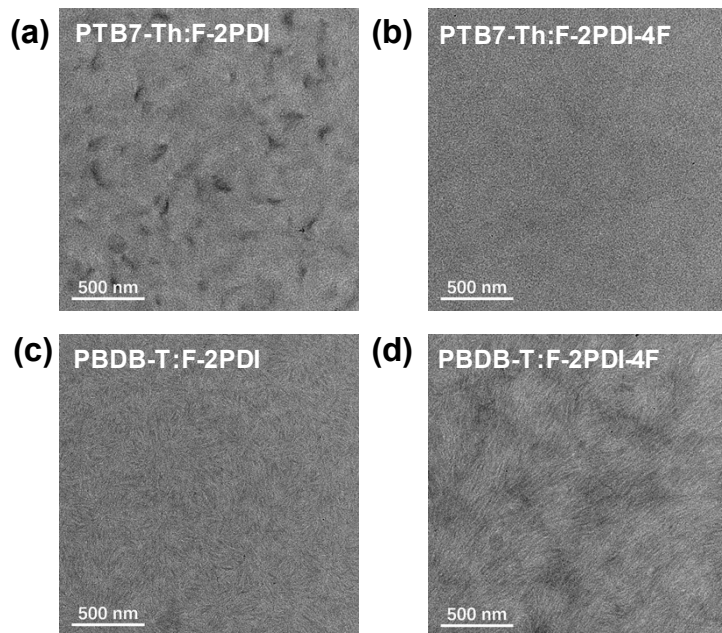


Fig. S6. TEM images ($2 \times 2 \mu\text{m}$) of blend films based on (a) PTB7-Th:F-2PDI, (b) PTB7-Th:F-2PDI-4F, (c) PBDB-T:F-2PDI, and (d) PBDB-T:F-2PDI-4F, respectively.

Table S5. Characteristic length scale of packing phenomenon in blend films of PTB7-Th:F-2PDI, PTB7-Th:F-2PDI-4F, PBDB-T:F-2PDI and PBDB-T:F-2PDI-4F, respectively.

active layer	Lamella Packing			$\pi-\pi$ Stacking		
	(100) distance [Å]	FWHM[Å ⁻¹]	CCL [Å]	$\pi-\pi$ distance [Å]	FWHM[Å ⁻¹]	CCL [Å]
PTB7-Th:F-2PDI	21.9 ^a	0.127	44.4	3.87 ^b	0.415	13.6
PTB7-Th:F-2PDI-4F	19.0 ^b	0.0773	73.2	3.90 ^b	0.442	12.8
PBDB-T:F-2PDI	21.5 ^a	0.0431	131	3.70 ^b	0.255	22.2
PBDB-T:F-2PDI-4F	20.3 ^a	0.0419	135	3.61 ^b	0.203	27.8

FWHM represents full-width at half maximum, CCL represents crystal coherence length, ^a Represents In-plane ^b represents Out-of-Plane.

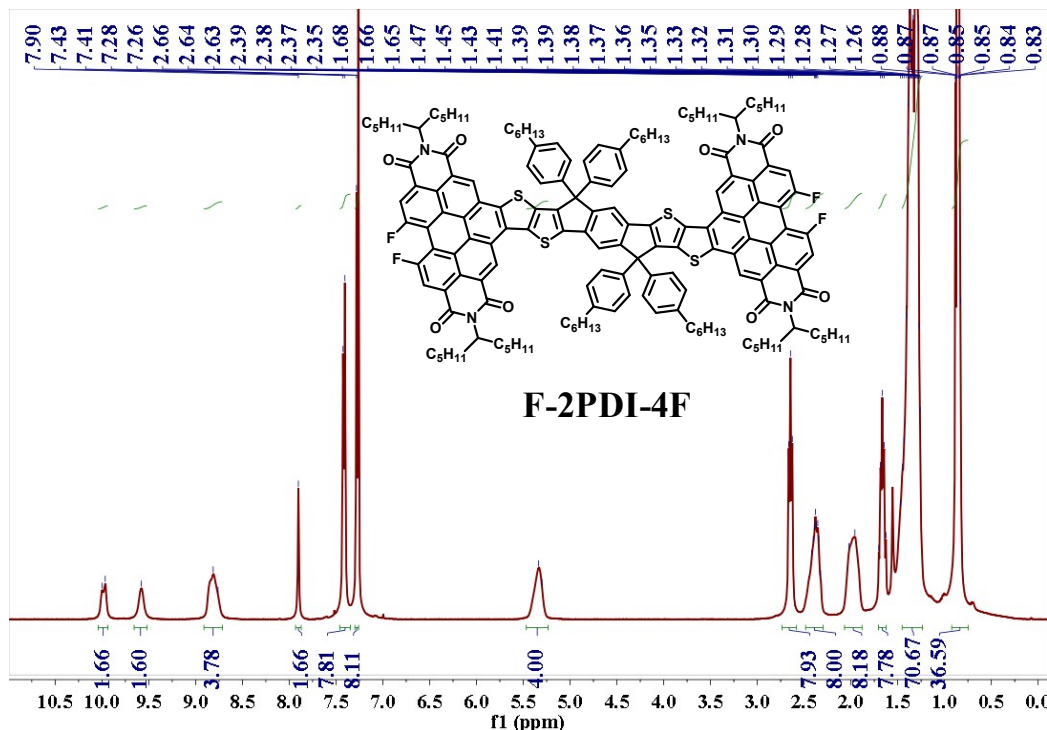


Fig. S7. ¹H NMR spectrum of F-2PDI-4F.

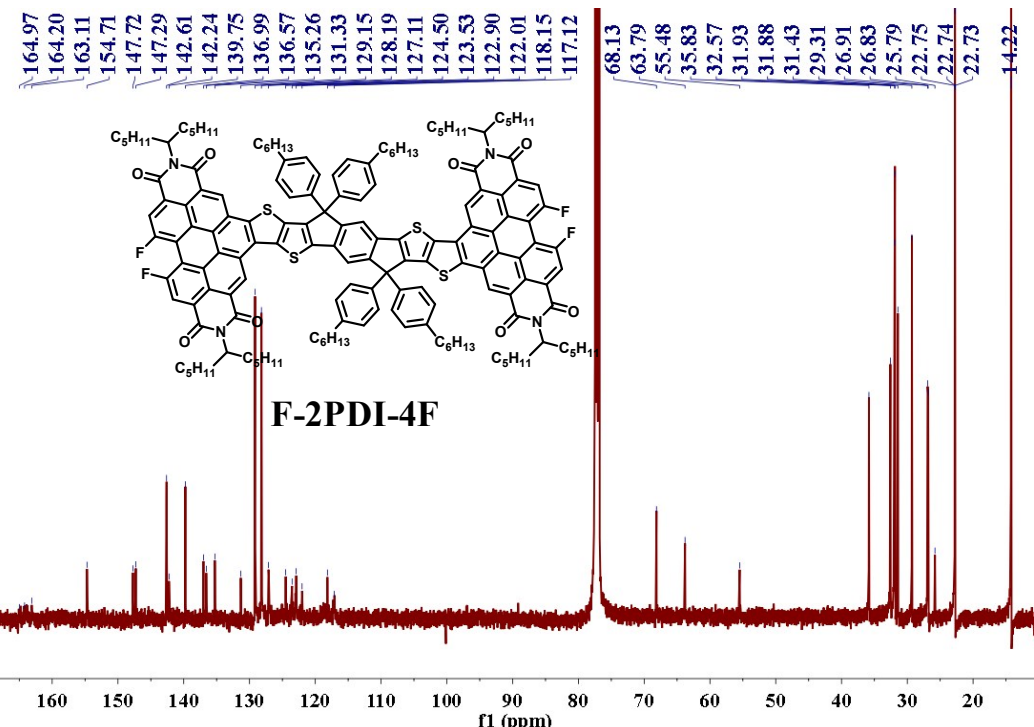


Fig. S8. ^{13}C NMR spectrum of F-2PDI-4F.

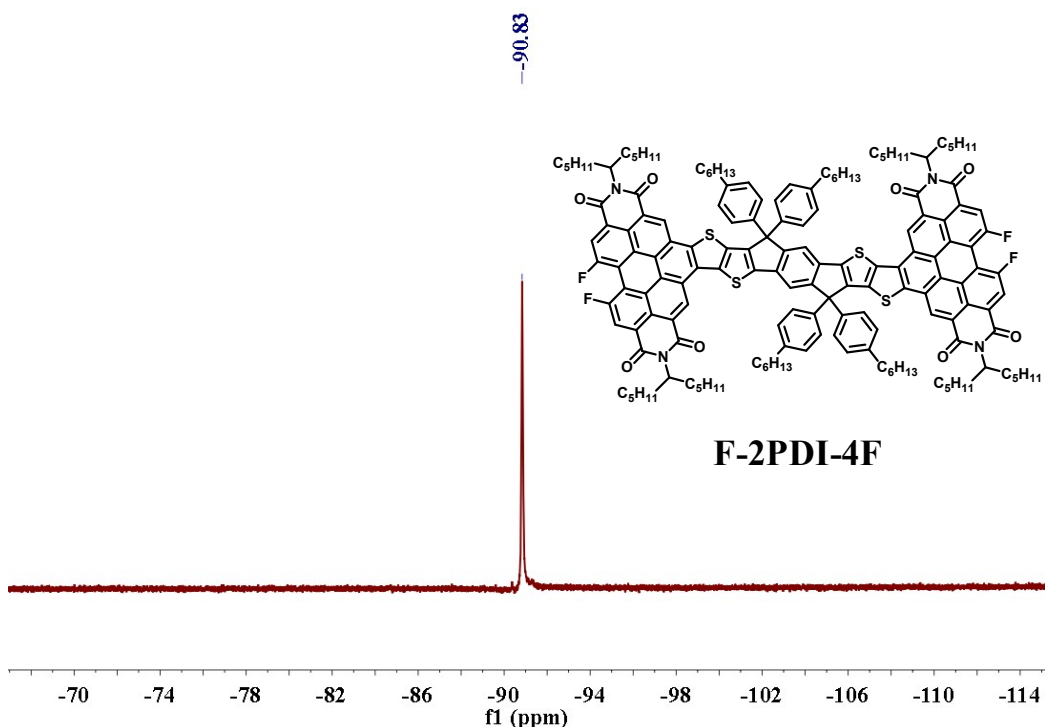


Fig. S9. ^{19}F NMR spectrum of F-2PDI-4F.

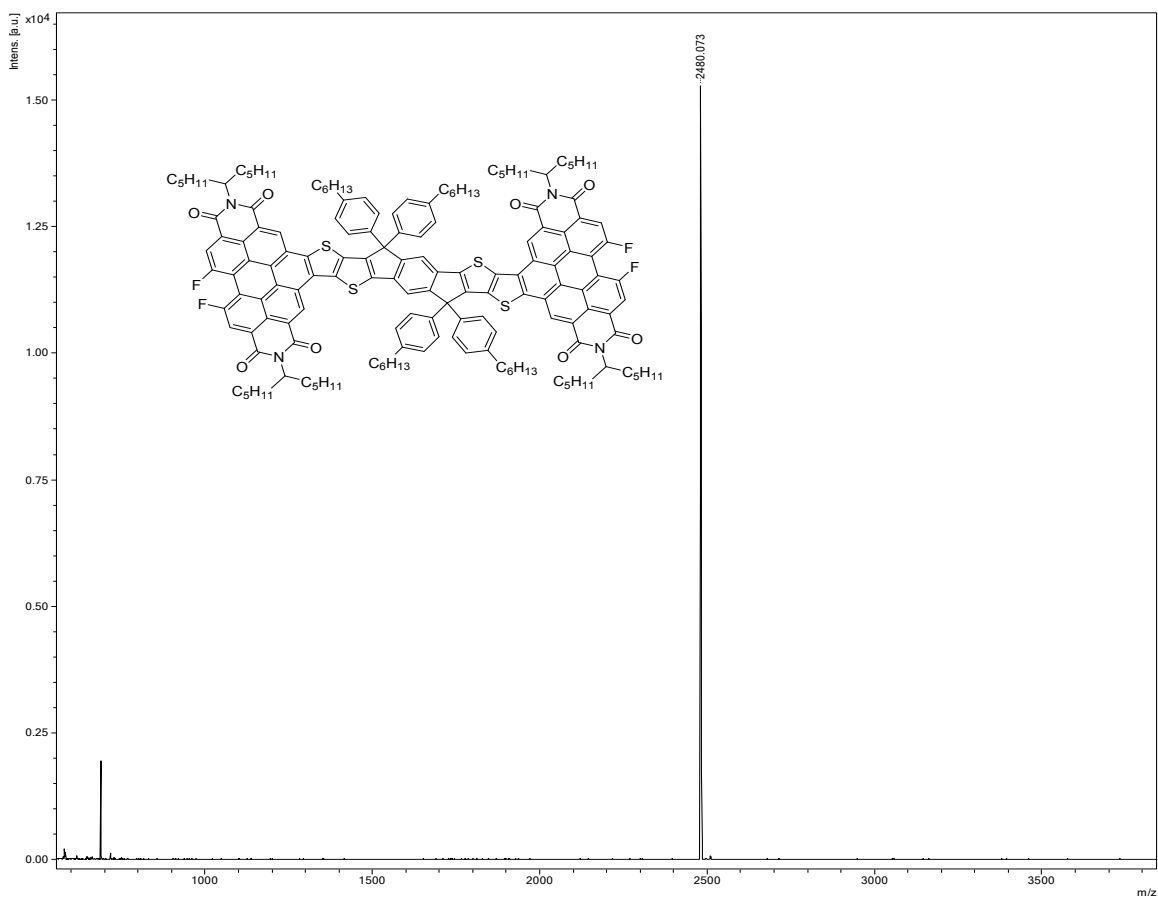


Fig. S10. Maldi-Tof-MS spectrum of F-2PDI-4F.

Reference

- Ziffer, M. E.; Jo, S. B.; Zhong, H.; Ye, L.; Liu, H.; Lin, F.; Zhang, J.; Li, X.; Ade, H. W.; Jen, A. K.; Ginger, D. S., Long-Lived, Non-Geminate, Radiative Recombination of Photogenerated Charges in a Polymer/Small-Molecule Acceptor Photovoltaic Blend. *J. Am. Chem. Soc.*, 2018, 140, (31), 9996-10008.
- Li, S. X.; Liu, W. Q.; Li, C. Z.; Lau, T. K.; Lu, X. H.; Shi, M. M.; Chen, H. Z., A Non-Fullerene Acceptor with a Fully Fused Backbone for Efficient Polymer Solar Cells with a High Open-Circuit Voltage. *J. Mater. Chem. A*, 2016, 4, (39), 14983-14987.
- Cai, Y. H.; Huo, L. J.; Sun, X. B.; Wei, D. H.; Tang, M. S.; Sun, Y. M., High Performance Organic Solar Cells Based on a Twisted Bay-Substituted Tetraphenyl Functionalized Perylenediimide Electron Acceptor. *Adv. Energy Mater.*, 2015, 5, (11), 1500032.
- Yi, J. D.; Wang, J. K.; Lin, Y.; Gao, W.; Ma, Y. C.; Tan, H. W.; Wang, H. Y.; Ma, C. Q., Molecular Geometry Regulation of Bay-Phenyl Substituted Perylenediimide Derivatives with Bulky Alkyl Chain for use in Organic Solar Cells as the Electron Acceptor. *Dyes Pigm.*, 2017, 136, 335-346.
- Chen, Y. X.; Zhang, X.; Zhan, C. L.; Yao, J. N., In-Depth Understanding of Photocurrent Enhancement in Solution-Processed Small-Molecule:Perylene Diimide Non-Fullerene Organic Solar Cells. *Phys. Status Solidi.*, 2015, 212, (9), 1961-1968.
- Sun, J. P.; Hendsbee, A. D.; Dobson, A. J.; Welch, G. C.; Hill, I. G., Perylene Diimide based All Small-Molecule Organic Solar Cells: Impact of Branched-Alkyl Side Chains on Solubility, Photophysics, Self-Assembly, and Photovoltaic Parameters. *Org. Electron.*, 2016, 35, 151-157.
- Wang, H. L.; Fan, Q. X.; Chen, L. C.; Xiao, Y., Amino-Acid Ester Derived Perylene Diimides Electron Acceptor Materials: An Efficient Strategy For Green-Solvent-Processed Organic Solar Cells. *Dyes Pigm.*, 2019, 164, 384-389.
- Cai, Z.; Zhao, D.; Sharapov, V.; Awais, M. A.; Zhang, N.; Chen, W.; Yu, L., Enhancement in Open-Circuit Voltage in Organic Solar Cells by Using Ladder-Type Nonfullerene Acceptors. *ACS Appl. Mater. Interfaces*, 2018, 10, (16), 13528-13533.

9. Zhao, D.; Wu, Q.; Cai, Z.; Zheng, T.; Chen, W.; Lu, J.; Yu, L., Electron Acceptors Based on α -Substituted Perylene Diimide (PDI) for Organic Solar Cells. *Chem. Mater.*, 2016, 28, (4), 1139-1146.
10. Xia, P.; Wu, M. L.; Zhang, S. X.; Hu, J.; Chen, L.; Bu, T. L.; Yi, J. P.; Wu, D.; Xia, J. L., High Performance PDI based Ternary Organic Solar Cells Fabricated with Non-Halogenated Solvent. *Org. Electron.*, 2019, 73, 205-211.
11. Sun, H.; Sun, P.; Zhang, C.; Yang, Y.; Gao, X.; Chen, F.; Xu, Z.; Chen, Z. K.; Huang, W., High-Performance Organic Solar Cells Based on a Non-Fullerene Acceptor with a Spiro Core. *Chem. Asian J.*, 2017, 12, (7), 721-725.
12. Yu, S.; Chen, Y.; Wu, J.; Xia, D.; Hong, S.; Wu, X.; Yu, J.; Zhang, S.; Peng, A.; Huang, H., Iris-Like Acceptor with Most PDI Units for Organic Solar Cells. *ACS Appl. Mater. Interfaces*, 2018, 10, (34), 28812-28818.
13. Hu, H. W.; Li, Y. K.; Zhang, J. Q.; Peng, Z. X.; Ma, L. K.; Xin, J. M.; Huang, J. C.; Ma, T. X.; Jiang, K.; Zhang, G. Y.; Ma, W.; Ade, H.; Yan, H., Effect of Ring-Fusion on Miscibility and Domain Purity: Key Factors Determining the Performance of PDI-Based Nonfullerene Organic Solar Cells. *Adv. Energy Mater.*, 2018, 8, (26), 1800234.
14. Duan, Y.; Xu, X.; Yan, H.; Wu, W.; Li, Z.; Peng, Q., Pronounced Effects of a Triazine Core on Photovoltaic Performance-Efficient Organic Solar Cells Enabled by a PDI Trimer-Based Small Molecular Acceptor. *Adv. Mater.*, 2017, 29, (7), 1605115.
15. Lin, Y.; Wang, Y.; Wang, J.; Hou, J.; Li, Y.; Zhu, D.; Zhan, X., A Star-Shaped Perylene Diimide Electron Acceptor for High-Performance Organic Solar Cells. *Adv. Mater.*, 2014, 26, (30), 5137-42.
16. Xiong, Y.; Wu, B.; Zheng, X.; Zhao, Z.; Deng, P.; Lin, M.; Tang, B.; Ong, B. S., Novel Dimethylmethyleno-Bridged Triphenylamine-PDI Acceptor for Bulk-Heterojunction Organic Solar Cells. *Adv. Sci.*, 2017, 4, (10), 1700110.
17. Yi, J.; Wang, Y.; Luo, Q.; Lin, Y.; Tan, H.; Wang, H.; Ma, C. Q., A 9,9'-Spirobi[9H-fluorene]-cored Perylenediimide Derivative and its Application in Organic Solar cells as a Non-Fullerene Acceptor. *Chem. Commun.*, 2016, 52, (8), 1649-52.
18. Meng, D.; Sun, D.; Zhong, C.; Liu, T.; Fan, B.; Huo, L.; Li, Y.; Jiang, W.; Choi, H.; Kim, T.; Kim, J. Y.; Sun, Y.; Wang, Z.; Heeger, A. J., High-Performance Solution-Processed Non-Fullerene Organic Solar Cells Based on Selenophene-Containing Perylene Bisimide Acceptor. *J. Am. Chem. Soc.*, 2016, 138, (1), 375-80.
19. Wu, M. L.; Yi, J. P.; Hu, J.; Xia, P.; Wang, H.; Chen, F.; Wu, D.; Xia, J. L., Ring Fusion Attenuates the Device Performance: Star-Shaped Long Helical Perylene Diimide based Non-Fullerene Acceptors. *J. Mater. Chem. C*, 2019, 7, (31), 9564-9572.
20. Jiang, W.; Ye, L.; Li, X.; Xiao, C.; Tan, F.; Zhao, W.; Hou, J.; Wang, Z., Bay-Linked Perylene Bisimides as Promising Non-Fullerene Acceptors for Organic Solar Cells. *Chem. Commun.*, 2014, 50, (8), 1024-6.
21. Duan, Y.; Xu, X.; Li, Y.; Li, Z.; Peng, Q., Chalcogen-Atom-Annulated Perylene Diimide Trimers for Highly Efficient Nonfullerene Polymer Solar Cells. *Macro. Rapid Commun.*, 2017, 38, (23), 1700405.
22. Wu, M.; Yi, J. P.; Chen, L.; He, G.; Chen, F.; Sfeir, M. Y.; Xia, J., Novel Star-Shaped Helical Perylene Diimide Electron Acceptors for Efficient Additive-Free Nonfullerene Organic Solar Cells. *ACS Appl. Mater. Interfaces*, 2018, 10, (33), 27894-27901.
23. Sun, D.; Meng, D.; Cai, Y.; Fan, B.; Li, Y.; Jiang, W.; Huo, L.; Sun, Y.; Wang, Z., Non-Fullerene-Acceptor-Based Bulk-Heterojunction Organic Solar Cells with Efficiency over 7%. *J. Am. Chem. Soc.*, 2015, 137, (34), 11156-62.
24. Zhang, J.; Li, Y.; Huang, J.; Hu, H.; Zhang, G.; Ma, T.; Chow, P. C. Y.; Ade, H.; Pan, D.; Yan, H., Ring-Fusion of Perylene Diimide Acceptor Enabling Efficient Nonfullerene Organic Solar Cells with a Small Voltage Loss. *J. Am. Chem. Soc.*, 2017, 139, (45), 16092-16095.
25. Nakano, M.; Nakano, K.; Takimiya, K.; Tajima, K., Two Isomeric Perylenothiophene Diimides: Physicochemical Properties and Applications in Organic Semiconducting Devices. *J. Mater. Chem. C*, 2019, 7, (8), 2267-2275.
26. Han, H.; Ma, L. K.; Zhang, L.; Guo, Y.; Li, Y.; Yu, H.; Ma, W.; Yan, H.; Zhao, D., Tweaking the Molecular Geometry of a Tetraperylenediimide Acceptor. *ACS Appl. Mater. Interfaces*, 2019, 11, (7), 6970-6977.
27. Wang, H. L.; Chen, L. C.; Xiao, Y., Constructing a Donor-Acceptor Linear-Conjugation Structure for Heterologous Perylene Diimides to Greatly Improve the Photovoltaic Performance. *J. Mater. Chem. C*, 2019, 7, (4), 835-842.
28. Liu, S. Y.; Wu, C. H.; Li, C. Z.; Liu, S. Q.; Wei, K. H.; Chen, H. Z.; Jen, A. K., A Tetraperylene Diimides Based 3D Nonfullerene Acceptor for Efficient Organic Photovoltaics. *Adv. Sci.*, 2015, 2, (4), 1500014.
29. Fan, W.; Liang, N.; Meng, D.; Feng, J.; Li, Y.; Hou, J.; Wang, Z., A High Performance Three-Dimensional Thiophene-Annulated Perylene Dye as an Acceptor for Organic Solar Cells. *Chem. Commun.*, 2016, 52, (77), 11500-11503.
30. Yang, L.; Gu, W.; Lv, L.; Chen, Y.; Yang, Y.; Ye, P.; Wu, J.; Hong, L.; Peng, A.; Huang, H., Triplet Tellurophene-Based Acceptors for Organic Solar Cells. *Angew. Chem., Int. Ed.*, 2018, 57, (4), 1096-1102.
31. Payne, A. J.; Song, J.; Sun, Y.; Welch, G. C., A Tetrameric Perylene Diimide Non-Fullerene Acceptor via Unprecedented Direct (Hetero)Arylation Cross-Coupling Reactions. *Chem. Commun.*, 2018, 54, (81), 11443-11446.
32. Zhan, X. J.; Xiong, W. T.; Gong, Y. B.; Liu, T.; Xie, Y. J.; Peng, Q.; Sun, Y. M.; Li, Z., Pyrene-Fused Perylene Diimides: New Building Blocks to Construct Non-Fullerene Acceptors With Extremely High Open-Circuit Voltages up to 1.26 V. *Solar Rrl*, 2017, 1, (10), 1700123.
33. Li, S. S.; Zhang, H.; Zhao, W. C.; Ye, L.; Yao, H. F.; Yang, B.; Zhang, S. Q.; Hou, J. H., Green-Solvent-Processed All-Polymer Solar Cells Containing a Perylene Diimide-Based Acceptor with an Efficiency over 6.5%. *Adv. Energy Mater.*, 2016, 6, (5), 1501991.
34. Li, X. L.; Wu, K. L.; Zheng, L. P.; Deng, Y. H.; Tan, S. T.; Chen, H. J., Synthesis and Characterization of Novel Benzodithiophene-Fused Perylene Diimide Acceptors: Regulate Photovoltaic Performance via Structural Isomerism. *Dyes Pigm.*, 2019, 168, 59-67.

35. Sun, H.; Song, X.; Xie, J.; Sun, P.; Gu, P.; Liu, C.; Chen, F.; Zhang, Q.; Chen, Z. K.; Huang, W., PDI Derivative through Fine-Tuning the Molecular Structure for Fullerene-Free Organic Solar Cells. *ACS Appl. Mater. Interfaces*, 2017, 9, (35), 29924-29931.
36. Zhong, H.; Wu, C. H.; Li, C. Z.; Carpenter, J.; Chueh, C. C.; Chen, J. Y.; Ade, H.; Jen, A. K., Rigidifying Nonplanar Perylene Diimides by Ring Fusion Toward Geometry-Tunable Acceptors for High-Performance Fullerene-Free Solar Cells. *Adv. Mater.*, 2016, 28, (5), 951-8.
37. Meng, D.; Fu, H.; Fan, B.; Zhang, J.; Li, Y.; Sun, Y.; Wang, Z., Rigid Nonfullerene Acceptors Based on Triptycene-Perylene Dye for Organic Solar Cells. *Chem. Asian J.*, 2017, 12, (12), 1286-1290.
38. Meng, D.; Fu, H.; Xiao, C.; Meng, X.; Winands, T.; Ma, W.; Wei, W.; Fan, B.; Huo, L.; Doltsinis, N. L.; Li, Y.; Sun, Y.; Wang, Z., Three-Bladed Rylene Propellers with Three-Dimensional Network Assembly for Organic Electronics. *J. Am. Chem. Soc.*, 2016, 138, (32), 10184-90.
39. Gao, G.; Liang, N.; Geng, H.; Jiang, W.; Fu, H.; Feng, J.; Hou, J.; Feng, X.; Wang, Z., Spiro-Fused Perylene Diimide Arrays. *J. Am. Chem. Soc.*, 2017, 139, (44), 15914-15920.
40. Fu, H. T.; Meng, D.; Meng, X. Y.; Sun, X. B.; Huo, L. J.; Fan, Y. Z.; Li, Y.; Ma, W.; Sun, Y. M.; Wang, Z. H., Influence of Alkyl Chains on Photovoltaic Properties of 3D Rylene Propeller Electron Acceptors. *J. Mater. Chem. A*, 2017, 5, (7), 3475-3482.
41. Liang, N. N.; Zhu, X. X.; Zheng, Z.; Meng, D.; Liu, G. G.; Zhang, J. Q.; Li, S. S.; Li, Y.; Hou, J. H.; Hu, B.; Wang, Z. H., Tuning Charge Generation Process of Rylene Imide-Based Solar Cells via Chalcogen-Atom-Annulation. *Chem. Mater.*, 2019, 31, (10), 3636-3643.
42. Li, X. C.; Wang, H. B.; Nakayama, H.; Wei, Z. T.; Schneider, J. A.; Clark, K.; Lai, W. Y.; Huang, W.; Labram, J. G.; de Alaniz, J. R.; Chabiny, M. L.; Wudl, F.; Zheng, Y. H., Multi-Sulfur-Annulated Fused Perylene Diimides for Organic Solar Cells with Low Open-Circuit Voltage Loss. *ACS Appl. Energy Mater.*, 2019, 2, (5), 3805-3814.
43. Zhong, Y.; Trinh, M. T.; Chen, R.; Purdum, G. E.; Khlyabich, P. P.; Sezen, M.; Oh, S.; Zhu, H.; Fowler, B.; Zhang, B.; Wang, W.; Nam, C. Y.; Sfeir, M. Y.; Black, C. T.; Steigerwald, M. L.; Loo, Y. L.; Ng, F.; Zhu, X. Y.; Nuckolls, C., Molecular Helices as Electron Acceptors in High-Performance Bulk Heterojunction Solar Cells. *Nat. Commun.*, 2015, 6, 8242.
44. Liu, J.; Chen, S. S.; Qian, D. P.; Gautam, B.; Yang, G. F.; Zhao, J. B.; Bergqvist, J.; Zhang, F. L.; Ma, W.; Ade, H.; Inganäs, O.; Gundogdu, K.; Gao, F.; Yan, H., Fast Charge Separation in a Non-Fullerene Organic Solar Cell with a Small Driving Force. *Nat. Energy*, 2016, 1, (7), 16089.
45. Zhang, J.; Bai, F.; Li, Y.; Hu, H.; Liu, B.; Zou, X.; Yu, H.; Huang, J.; Pan, D.; Ade, H.; Yan, H., Intramolecular π -Stacked Perylene-Diimide Acceptors for Non-Fullerene Organic Solar Cells. *J. Mater. Chem. A*, 2019, 7, (14), 8136-8143.
46. Cheng, J. R.; Li, B.; Ren, X. J.; Liu, F.; Zhao, H. C.; Wang, H. J.; Wu, Y. G.; Chen, W. P.; Ba, X. W., Highly Twisted Ladder-Type Backbone Bearing Perylene Diimides for Non-Fullerene Acceptors in Organic Solar Cells. *Dyes Pigm.*, 2019, 161, 221-226.
47. Luo, Z.; Liu, T.; Chen, Z.; Xiao, Y.; Zhang, G.; Huo, L.; Zhong, C.; Lu, X.; Yan, H.; Sun, Y.; Yang, C., Isomerization of Perylene Diimide Based Acceptors Enabling High-Performance Nonfullerene Organic Solar Cells with Excellent Fill Factor. *Adv. Sci.*, 2019, 6, (6), 1802065.
48. Zhang, G.; Feng, J.; Xu, X.; Ma, W.; Li, Y.; Peng, Q., Perylene Diimide-Based Nonfullerene Polymer Solar Cells with over 11% Efficiency Fabricated by Smart Molecular Design and Supramolecular Morphology Optimization. *Adv. Funct. Mater.*, 2019, 1906587.
49. Wang K, Xia P, Wang KW, et al. (2020), Pi-extension, selenium incorporation, and trimerization: "Three in one" for efficient perylene diimide oligomer-based organic solar cells. *ACS Appl. Mater. Interfaces*, 2020 12: 9528-9536.
50. Liu, J.; Lu, H.; Liu, Y.; Zhang, J.; Li, C.; Xu, X.; Bo, Z., Efficient Organic Solar Cells Based on Non-Fullerene Acceptors with Two Planar Thiophene Fused Perylene Diimide Units. *ACS Appl. Mater. Interfaces*, 2020, 12, (9), 10746-10754
51. H. Yu, L. Arunagiri, L. Zhang, J. Huang, W. Ma, J. Zhang and H. Yan, Transannularly conjugated tetrameric perylene diimide acceptors containing [2.2]paracyclophane for non-fullerene organic solar cells. *J. Mater. Chem. A*, 2020, 8, 6501-6509.
52. Z. Lu, B. Jiang, X. Zhang, A. Tang, L. Chen, C. Zhan and J. Yao, Perylene-Diimide Based Non-Fullerene Solar Cells with 4.34% Efficiency through Engineering Surface Donor/Acceptor Composition. *Chem. Mater.*, 2014, 26, 2907-2914.
53. T. Ye, S. Jin, C. Kang, C. Tian, X. Zhang, C. Zhan, S. Lu and Z. Kan, Comparison Study of Wide Bandgap Polymer (PBDB-T) and Narrow Bandgap Polymer (PBDTTT-EFT) as Donor for Perylene Diimide Based Polymer Solar Cells. *Front. Chem.*, 2018, 6, 613.
54. J. Pan, L. Wang, W. Chen, S. Sang, H. Sun, B. Wu, X.-C. Hang, Z. Sun and W. Huang, Non-fullerene small molecule acceptors with three-dimensional thiophene/selenopheneannulated perylene diimides for efficient organic solar cells. *J. Mater. Chem. C*, 2020, DOI: 10.1039/d0tc00341g.